

A Multi-scale Residual Transformer for VLF Lightning Transients Classification

Jinghao Sun¹, Tingting Ji^{*2}, Guoyu Wang³, and Rui Wang⁴

¹Faculty of Information Science and Engineering, Ocean University of China, Qingdao, China

²Teaching Center of Fundamental Courses, Ocean University of China, Qingdao, China

³Faculty of Information Science and Engineering, Ocean University of China, Qingdao, China

⁴Physics and Electronic Information, Yantai University, Yantai, China

Abstract—The utilization of Very Low Frequency (VLF) electromagnetic signals in navigation systems is widespread. However, the non-stationary behavior of lightning signals can affect VLF electromagnetic signal transmission. Accurately classifying lightning signals is important for reducing interference and noise in VLF, thereby improving the reliability and overall performance of navigation systems. In recent years, the evolution of deep learning, specifically Convolutional Neural Network (CNNs), has sparked a transformation in lightning classification, surpassing traditional statistical methodologies. Existing CNN models have limitations as they overlook the diverse attributes of lightning signals across different scales and neglect the significance of temporal sequencing in sequential signals. This study introduces an innovative multi-scale residual transform (MRTransformer) that not only has the ability to discern intricate fine-grained patterns while also weighing the significance of different aspects within the input lightning signal sequence. This model performs the attributes of the lightning signal across different scales and the level of accuracy reached 90% in the classification. In future work, this model has the potential applied to a comprehensive understanding of the localization and waveform characteristics of lightning signals.

Index Terms—VLF electromagnetic signal, lightning signal, lightning waveform characteristics, classification, and the multi-scale residual transform model.

I. INTRODUCTION

VERY low frequency (VLF) [1] [44] refers to long-wave communication using radio waves ranging between 3kHz and 30kHz (wavelengths from 100km to 10km). In comparison to communication operating within the microwave frequency range, terrestrial long-wave communication within the VLF band presents distinct advantages. These include channel stability, extended propagation distances, capacity for water penetration, and the ability to navigate intricate terrain. Such advantages have found wide-ranging applications across diverse domains [18, 26, 45, 46], spanning submarine communication to satellite navigation systems.

Leveraging VLF electromagnetic signals offers a notably stable approach to remote sensing. However, as these signals propagate through the 'earth-ionosphere wave-guide,' atmospheric noise interference arising from various activities emerges as a primary challenge for VLF signals [8, 9, 30, 47, 49]. Among these sources, lightning discharges proximate to

the signal receiver emerge as the most substantial interference source. Lightning impulses introduce non-stationary characteristics within VLF, consequently diminishing communication quality and impacting navigational positioning accuracy. The classification of lightning events allows for capturing the fundamental waveform features of nearby lightning impulses, serving as the focal point in research endeavors pertaining to lightning signal detection, localization, and the enhancement of communication quality within VLF sensing.

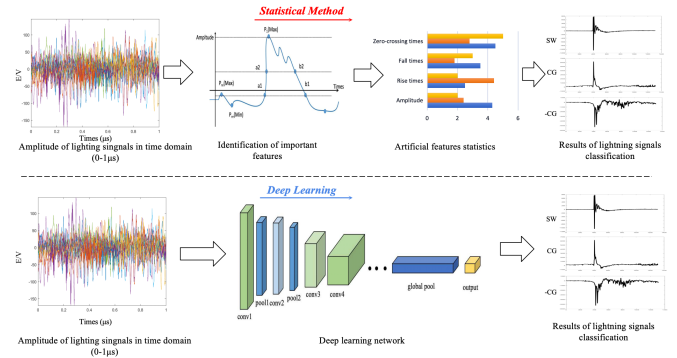


Fig. 1: The comparison schema for statistical method and deep learning

VLF sensing and the Time of Arrival (TOA) method have played a crucial role in lightning location systems. Traditionally, statistical methods have been used to determine important features of VLF waveforms, such as amplitude, rise and fall times, zero-cross times, etc [11] [2]. However, in practical applications, there is a wide range of lightning types and a large amount of data to handle. The multi-parameter method faces challenges in extracting characteristic parameters from low-amplitude VLF signals, often resulting in the neglect of these smaller signals and reducing detection efficiency [4] [5]. Moreover, the characteristic parameters used in the multi-parameter method may vary across regions with different meteorological conditions [6, 7, 10, 17]. Therefore, the multi-parameter method is not an ideal approach for lightning signal classification. As shown in Fig.1, deep learning networks are introduced to improve the classification efficiency of lightning VLF/LF signals, particularly in managing intricate datasets and elevating classification precision. The deep learning techniques

*Corresponding author Email address: tinaji_ouc@163.com

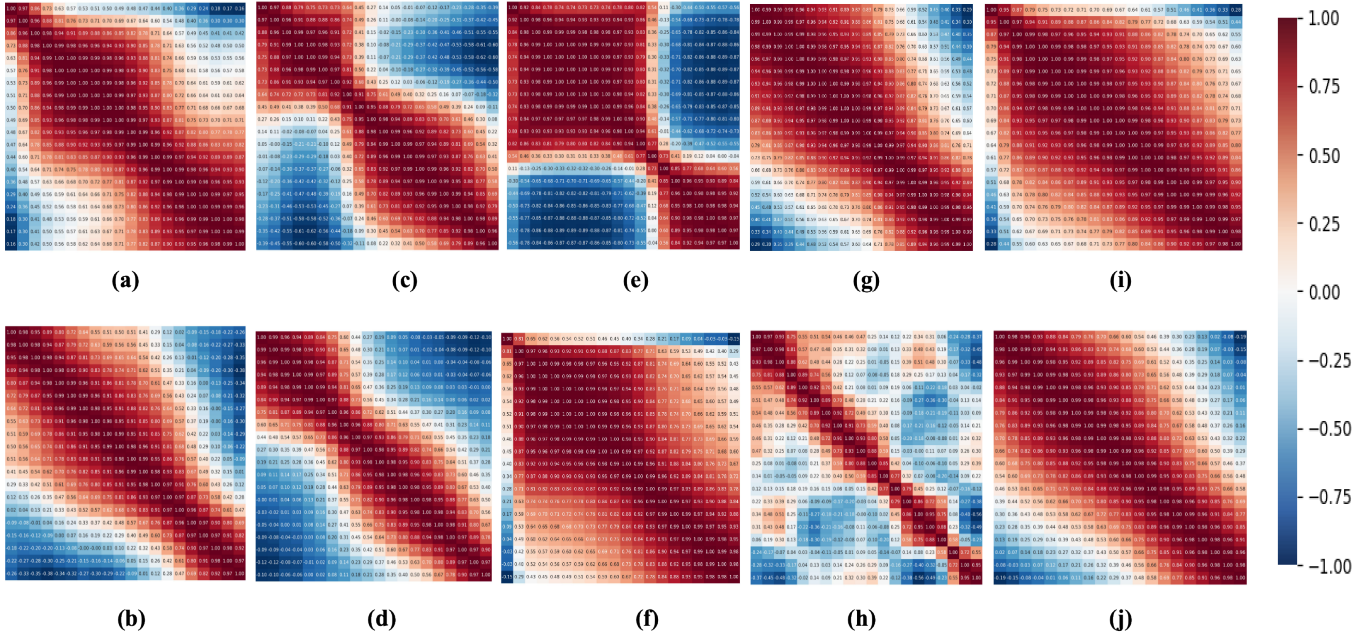


Fig. 2: The correlation heatmaps of lighting signals:(a)negative cloud-to-ground flash(-CG);(b)positive cloud-to-ground flash(+CG);(c)negative pre-breakdown(-PBP);(d)positive PBP(+PBP);(e)negative narrow bipolar envet(-NBE);(f)positive NBE(+NBE);(g)NBE;(h)multi-pulse cloud flash(MP);(i)cloud ground flash with ionosphere reflected signals(CG-IR);(j)skywave(SW).

for the classification of lightning events remain a relatively unexplored domain. Previous studies have much more effect on classifying lightning signals by using CNN networks and that with different structures. [14] [15] [21]. [22] gave an explanation for CNN networks. While these studies have ignored the impact of long-range dependencies in lightning sequences, understanding the relationships between distant parts of the signal is an essential part of classifying the lightning signals. There have also been previous studies [52] [53] that have explored the use of time-series-related methods for predicting lightning signals. It has been observed, as shown in Fig.2, that a majority of lightning signals display a strong correlation in the time series. Therefore, considering the correlation in time series is a key factor in the classification of lightning signals.

This article proposes a *multi-scale residual transformer* (MSRT) model to classify VLF lightning signals. The architecture comprises a multi-scale model with a connected residual and transformer model. To train this model, an open-source dataset including ten types of lightning signals was established for model training. Subsequently, The classification accuracy of the proposed model was compared with state-of-the-art methods using F1 score as evaluation criteria. To ensure a comprehensive comparison, we assessed the classification accuracy of each type by employing the Receiver Operating Characteristic curve analysis for two selected categories of lightning signals. In the ablation study, we utilized 5-fold cross-validation to assess the performance of our model. Additionally, we compared our model’s performance to that of a transformer-based model using accuracy and F1 score as met-

rics. To provide further insight into our model’s performance, we visualized the lightning features at each multi-scale layer using histograms. Finally, the generalization of the proposed model was tested on a dataset collected from Xinjiang.

In essence, this paper presents three significant contributions. Firstly, it introduces a multi-scale residual module that effectively captures information across multiple scales. This module enhances the model’s capability to discern local nuances within lightning signals at varying scales and skillfully integrates them to capture the overarching characteristics of lightning signals. Secondly, the paper combines the multi-scale residual module with a transformer model, marking the first instance of integration in VLF lightning signal classification. Furthermore, this approach takes into account the long-range dependencies present at each point of the lightning signal sequence.

II. THE RELATED WORK

A. The Related Lightning Signal Classification Work

Lightning, a dynamic atmospheric discharge, [48] [6]generates electromagnetic radiation detectable in the VLF. Harnessing this phenomenon for lightning detection and location is crucial for minimizing risks associated with lightning strikes. Based on the location where lightning is produced, lightning can be divided into two types: cloud-to-ground lightning (CG) and cloud lightning (CC). [50] [51] CG refers to lightning that occurs between thunderclouds and the earth or objects on the earth. CC refers to the entire process

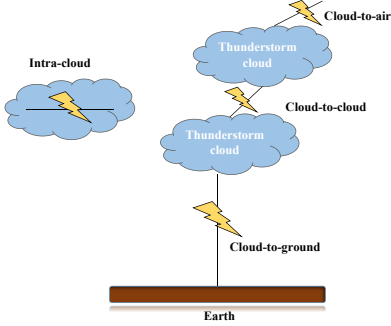


Fig. 3: The multiple types of lightning such as ground wave, sky wave, and wave conduction.

of lightning discharge without contacting objects on the ground. Such as the Fig.3 below, CC can be further divided into inter-cloud lightning, intra-cloud lightning, and cloud-air lightning. These emissions provide a unique signature that can be exploited for lightning detection and classification.

Classifying lightning events accurately is a pivotal challenge in lightning detection. The study [23] on waveform correlation of lightning pulses in VLF found that lightning strikes in this frequency range typically exhibit oscillating short pulses with multiple peaks and valleys, lasting from 1 to 10 milliseconds. Malan [25] used optical instruments and photography to study ground lightning and discovered that a single ground lightning is composed of multiple pulses, each lasting from several to tens of milliseconds, with a total duration of about 0.2 seconds. Alpert [27] and Challinor [28] also recorded transient photography of lightning pulses in the VLF range.

Traditional methods employ multi-parameter criteria [12, 14], but these often struggle with low-amplitude signals and variations across meteorological conditions. The need for precise classification is underscored by the potential consequences of misclassification, making it imperative to discern between CGs, ICs, and other events like narrow bipolar events (NBEs) [36, 40, 41].

In recent years, machine learning methods, such as Support Vector Machines (SVM) and Convolutional Neural Networks (CNNs) [14, 15, 29, 38], especially [22] proposed an interpretable CNN have gained prominence in lightning signal classification. However, the existing CNN models have not fully considered the different characteristics of lightning signals at different scales and the temporal correlation of lightning signals.

The field of lightning signal processing is rapidly evolving, and the accurate classification of lightning events remains a focal point. Advancements in deep learning techniques hold promise, but the challenges of data imbalance and regional variability must be addressed. Developing multi-scale learning models can bridge the gap between features and long-range dependencies in lightning sequences to accommodate the diversity of lightning environments, enable reliable lightning event classification, and ultimately improve the effectiveness of lightning detection systems.

B. The Role of Deep Learning Classification Networks

Deep learning classification networks [3, 13, 37] have a broad and impactful role in various application areas beyond lightning signal processing. They excel in tasks like image classification [42], object recognition [19, 20], and medical diagnosis by recognizing patterns in data that might be missed by humans. These networks also play a crucial role in the natural language processing [43], object detection [13], and re-identification [24, 38]. For example, Graph interactive Transformer (GiT) [39] proposes a structure where graphs and transformers interact constantly, enabling close collaboration between global and local features for vehicle re-identification. Hybrid Pyramidal Graph Network (HPGN) [31] proposes a novel pyramid graph network targeting features, which is closely connected behind the backbone network to explore multi-scale spatial structural features. Hierarchical Similarity Graph Module (HSGM) [16] proposes a hierarchical similarity graph module to relieve the conflict of backbone networks and mine the discriminative features.

Additionally, deep learning networks contribute to drug discovery, environmental monitoring, and quality control in manufacturing. Overall, deep learning classification networks have transformative potential across a wide range of fields and industries. Their ability to extract meaningful patterns from complex data has led to advancements in automation, accuracy, and efficiency in various applications.

III. METHODS

MSRT is a CNN-Transformer hybrid signal classification model, which can simultaneously learn global and local feature representations and capture long-range information at ease. Concretely, MSRT mainly consists of two parts: the Multi-scale Residual Module is designed to extract local features of the input signal. The transformer Module captures global information. The overall framework is depicted in Fig.4.

A. The Classical Classification Networks

CNN networks have a wide range of applications in classification, but they also have certain limitations. Firstly, CNN networks face problems such as gradient vanishing, gradient explosion, or network degradation, leading to insufficient model generalization ability. Therefore, He et al. [33] proposed the ResNet structure based on residual blocks and achieved highly competitive classification results on multiple datasets.

Secondly, each convolutional layer has the same size as the convolutional kernel, which makes it difficult to handle the possible multi-scale features in the lightning waveform.

Finally, CNN networks not consider the temporal correlation of time sequence signals. In 2017, the Google research team proposed the Transformers architecture based on the self-attention mechanism [34], which showed great advantages in sequence modeling. Then, the Shifted Window Multi-Head Attention (SW-MSA) is used to achieve information fusion between non-overlapping windows.

Hence, in this paper, to address the limitation of CNN networks, there is a multi-scale transformer network proposed.

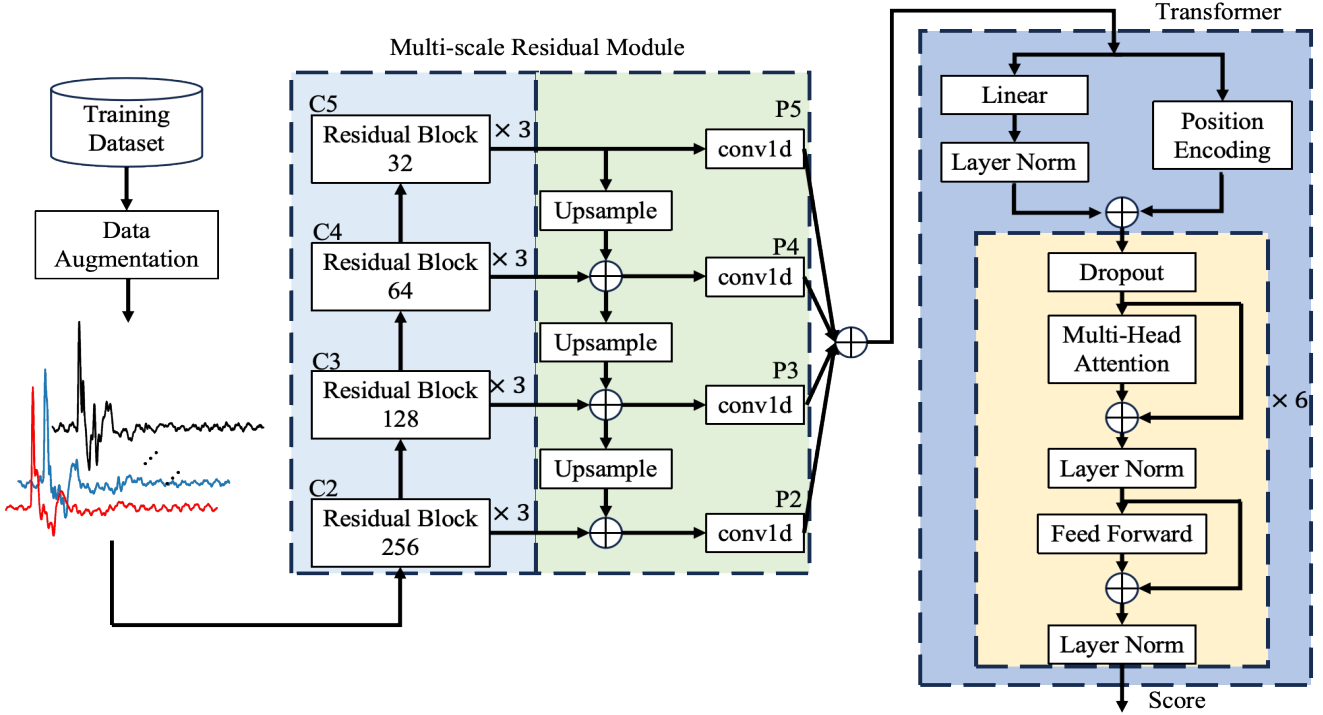


Fig. 4: The proposed model structure is as follows: Steps 1-3 describe the input waveform to the multi-scale module, which is then connected to the residual model through the transformer model. Finally, the model outputs the classification.

B. The Multi-scale Residual Transformer Structure

As shown in Fig.4, the model consists of several components, each playing a crucial role in ensuring its effectiveness. One of these components is the *multi-scale residual* (MSR) model, which is designed with residual parts to capture information at multiple scales. The MSR network architecture uses a Feature Pyramid Network (FPN) [54] backbone on top of a feedforward ResNet architecture to generate a rich feature pyramid. This model adeptly tackles this challenge by intelligently capturing information at multiple scales, ensuring that no crucial detail goes unnoticed. By integrating these diverse features, the model becomes capable of making decisions that are not only well-informed but also consider the holistic character of the signals under analysis. This feature integration mechanism is particularly beneficial in scenarios where signals manifest intricate patterns across different scales, enhancing the overall classification accuracy.

After the MSR, the transformer encoder is employed to handle long-range dependencies of each point of lighting signal sequences. The Transformer Encoder, with its inherent self-attention mechanisms, offers a solution to the complexities posed by long-range dependencies within lighting signal sequences. These self-attention mechanisms enable the model to weigh different parts of the input sequence, facilitating better contextual understanding and capturing intricate patterns within the data. By utilizing attention mechanisms, the transformer encoder can identify subtle relationships within the signal data, leading to accurate classification results.

The transformer encoder module consists of two parts:

1) a multi-head self-attention mechanism after a layer normalization, and 2) a multi-layer perceptron after multi-head self-attention and a layer normalization. In addition, in order to capture rich feature information, a residual connection is employed to connect these parts. The self-attention can be calculated as:

$$Attention(Q, K, V) = SoftMax\left(\frac{QK^T}{\sqrt{d}}\right)V \quad (1)$$

As shown in Fig.4, the multi-head attention comprises 6 self-attention blocks. After multi-head attention, the Feed-Forward Network (FFN) presents the capability to leverage local context. Following the intricate processing of features, the architecture employs a layer normalization step. This step ensures that the intermediate outputs remain consistent and well-behaved throughout the network. Layer normalization not only contributes to the stability of the training process but also enhances the overall speed of convergence.

Finally, the model employs a Linear fully connected layer as the final component to generate the classification output. This layer plays a crucial role in bridging the processed features and the desired classification outcome.

C. The Multi-scale Residual Module

As shown in Fig.4, the MSR is an essential component of the proposed model architecture, designed to capture information at multiple scales. We adopt the Feature Pyramid Network (FPN) as the backbone network for the MSR, build FPN on top of the Residual Network. The MSR module constructs

a rich and multi-scale feature pyramid from a 1D signal by incorporating a top-down pathway and lateral connections. As the Equation 2 description as:

$$C^{i+1} = \mathcal{F}(x, \{w_i\}) \quad (2)$$

Where C^{i+1} is defined as the output of the residual block, x is defined as the input lightning signal. $\mathcal{F}(x, \{w_i\})$ represents the residual mapping to be learned. The purpose of these residual layers is to downsample the input data and prevent gradients from disappearing.

The MSR extracts the features ranging from P2 to P5 of the feature pyramid. Description as the Equation 3:

$$P^i = \text{conv1D}(w_i, [\text{Upsampling}(C^{i+1}) + C^i]) + b^i \quad (3)$$

Where P^i is the output of the i layer, C^{i+1} through *Upsampling* layer to extend the output length. The upsampling operation aligns features from different scales, ensuring that information from multiple scales is combined effectively. Then multiply with C^i , which is through convolution. w_i is the multi-size convolution kernels at layer i . b^i is defined as the bias layer i . The output is the result of integrating the multi-scale features of each layer. This pathway allows the model to improve its understanding of the signal by first processing higher-level information, which then guides the processing of lower-level details. This iterative refinement mechanism enables the model to progressively fine-tune its understanding, leading to more accurate feature extraction.

IV. DATASET DESCRIPTION

A. The Experimental Dataset

In the experiment, we utilized the dataset from reference[14]. The open-source lightning data used in this study was collected by the Institute of Electrical Engineering, Chinese Academy of Sciences, using the advanced direction-time lightning detection system (ADTD). This system encompasses 333 detection stations across China and Southeast Asia, equipped with a channel bandwidth of 3 kHz to 400 kHz. The system's GPS time synchronization accuracy is within 20 ns, ensuring precise event timestamps. For locations with waveform acquisition, trigger sampling is employed. This method achieves a sampling rate of 1 MSPS, capturing lightning characteristics with 1 ms precision. Additionally, a pre-trigger sampling window of 100 μ s captures data leading up to the lightning event. According to reference, these signals were further divided into 10 types: negative cloud-to-ground flash (-CG), positive cloud-to-ground flash (+CG), negative pre-breakdown (-PBP), positive PBP (+PBP), negative narrow bipolar envet (-NBE), positive NBE (+NBE), NBE, multi-pulse cloud flash (MP), cloud ground flash with ionosphere reflected signals (CG-IR) and skywave (SW). Fig. 5 shows the typical waveforms of these types. The total number of signal samples that have been used is around 12000.

B. Testing Dataset Description

1) *The Testing Dataset:* The Yili of Xinjiang was studied using the GMS-08e electromagnetic instrument, and actual

data was obtained. The MFS-07e magnetic field sensor was utilized with a 50KHz bandwidth for every 1000 seconds. The VLF data collection system, shown in Fig. 6, featured the ADU-08e host in the middle, the Hx and Hy long bars as magnetic field sensors aligned in the north-south and east-west directions, and four small cylinders as non-polarized electrodes. The data acquisition equipment was set to a sampling rate of 131072Hz. In the implement experiment, the real data manually set a threshold of 500 millivolts was categorized as CG, CC, NBE, MP, or others in a total around of 900 data instances.

2) *Testing Dataset Preprocessing:* The noise in the data acquired and stored by ADU-08e can be categorized into two distinct components. The first component is situated in the high-frequency band (greater than 30kHz) and emanates from the sampling frequency. To effectively eliminate this, the implementation of a low-pass filter is recommended. The second component pertains to the low-frequency band (less than 1000Hz). Illustrated in Fig.7(a) and (b), this lower frequency range's noise primarily comprises a DC component and a 50Hz power frequency, along with its harmonics.

To obtain relatively clean VLF signal data from the initial configuration of the magnetometer MFS-07e, we employ averaging to remove the DC component, while a low-pass filter is utilized to discard noise beyond the very low-frequency range. Furthermore, a notch filter is applied to effectively remove the 50Hz power frequency and its harmonic interferences. These processes collectively constitute the preprocessing steps employed on the original captured data. The result of preprocessing is shown in Fig.7(c).

V. EXPERIMENTATION AND VALIDATION

A. Implementation Details

TABLE I: The hyperparameters used for training

Hyperparameter	Value
Batch Size	10
Epoch	12
Loss Function	CrossEntropy
Optimizer	Adam
Learning Rate	0.0001
Momentum	0.5

The essential hyperparameters outlined in this paper are presented in Table I. In this scenario, the batch size of the model processes 10 data samples, each comprising 1000 data points. The parameter epoch is 12, indicating that the model undertakes 12 complete iterations of forward and backward calculations. Notably, the epoch of the proposed method is roughly less than half the value employed in CNN models.

The model adopts the Cross-Entropy function for its loss computation and employs the Adam optimization algorithm. Following preliminary testing, the Learning Rate is set at 0.01, and Momentum is set to 0.5. These values collectively wield influence over the model's convergence rate and operational efficiency.

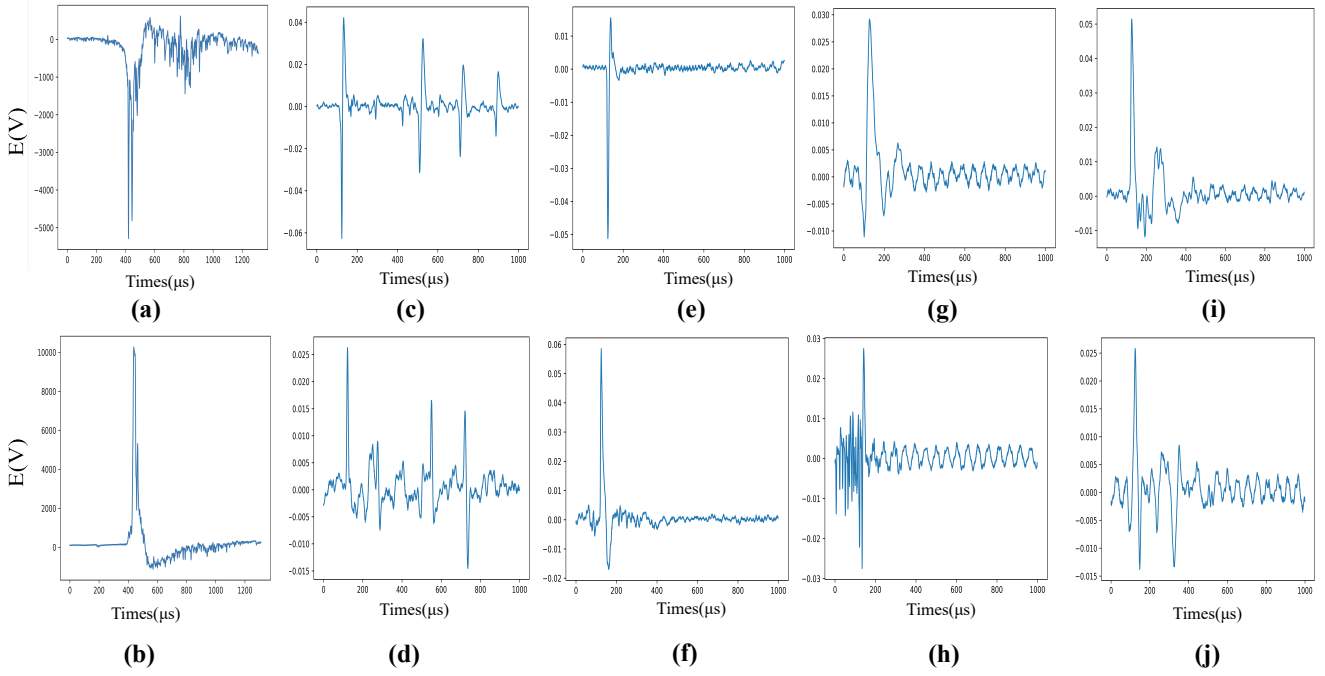


Fig. 5: The 10 types of signals: (a)negative cloud-to-ground flash (-CG); (b)positive cloud-to-ground flash (+CG); (c)negative pre-breakdown (-PBP); (d)positive PBP(+PBP); (e)negative narrow bipolar envet(-NBE); (f)positive nbe(+NBE); (g)NBE; (h)multi-pulse cloud flash (MP); (i)cloud ground flash with ionosphere reflected signals (CG-IR); (j)skywave(SW).

TABLE II: The F1 score results of SOTA

Types	Res	FPN	-CG(%)	CG-IR(%)	NBR(%)	+CG(%)	MP(%)	+PBP(%)	-PBP(%)	-NBE(%)	+NBE(%)	SW(%)	AVG(%)
CNN	no	no	0.0	70.0	80.0	83.0	80.0	88.0	74.0	87.0	90.0	84.0	76.0
	yes	no	85.0	84.0	86.0	95.0	93.0	94.0	85.0	93.0	95.0	90.0	90.0
	yes	yes	86.0	88.0	85.0	96.0	92.0	94.0	87.0	94.0	95.0	90.0	91.0
Transformer	no	no	83.0	81.0	78.0	92.0	86.0	88.0	78.0	91.0	89.0	89.0	86.0
	yes	no	83.0	82.0	82.0	81.0	82.0	87.0	73.0	85.0	92.0	90.0	89.0
	yes	yse	88.0	88.0	85.0	95.0	97.0	95.0	88.0	94.0	94.0	93.0	92.0

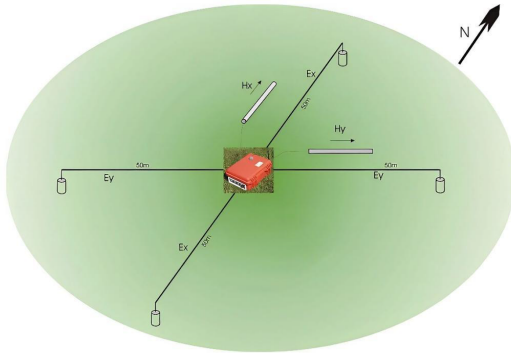


Fig. 6: The receiver for our implement dataset

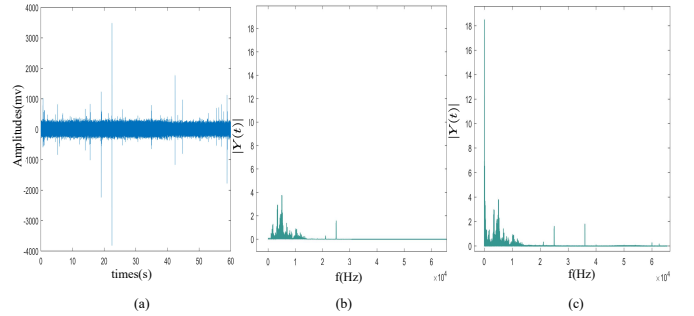


Fig. 7: The results of preprocessing:(a) the original lighting signal;(b)the frequency domain before pre-processing;(c) the frequency domain after preprocessing

B. Comparison with State-of-the-art Methods

In this section, our method comparison with *State-of-the-art* (SOTA) methods by using the experimental dataset and the F1-score as valuation criteria 4, which also known as the balanced score, is defined as the harmonic mean of precision

and recall.

$$F1 = 2 \cdot \frac{precision \cdot recall}{precision + recall} \quad (4)$$

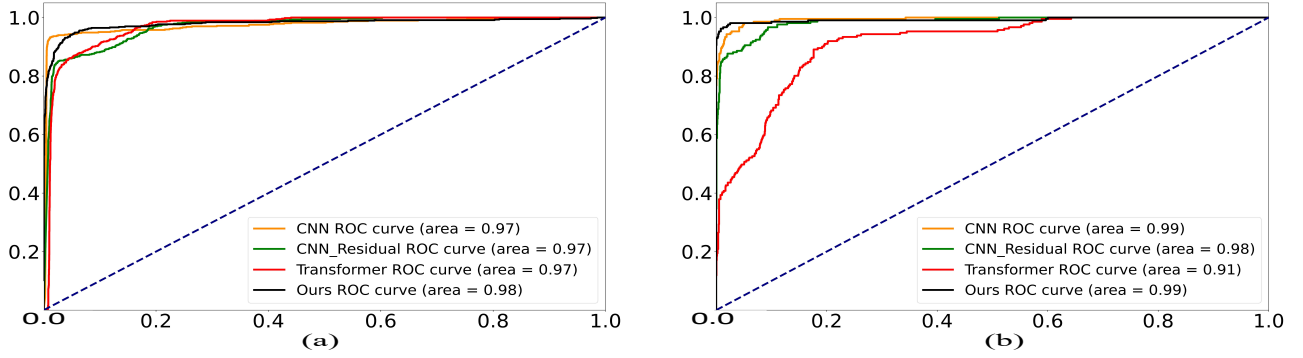


Fig. 8: The comparison ROC for different lighting signals:(a) the ROC of CG lighting;(b)the ROC of -NBE lighting

Where the *precision* represents the accuracy of predictions in the positive results of the sample. The *recall* represents the proportion of true positive samples that are predicted correctly out of all actual positive samples in the sample set.

The function of the average F1 score is definite as:

$$\text{AverageF1} = \frac{\sum F1score}{\text{Number_of_Epoch}} \quad (5)$$

Where $\sum F1score$ is the sum of the F1 score for each epoch, and the *Number_of_Epoch* is the total number of epochs for training.

1) *Comparison with F1 score:* Table II provides a comprehensive view of the average F1 scores achieved by state-of-the-art models for various types of lightning signals, all trained under the same epoch setting (epoch = 12). The models considered in the analysis encompass a spectrum of architectures, including the baseline CNN, CNN augmented with a residual module, CNN with both a residual and FPN module, Transformer, Transformer with a residual module, and our novel proposed method.

In both CNN and Transformer networks, the incorporation of residual connections and FPN modules improves the ability of signal classification. This observed improvement can be attributed to the intrinsic advantages of residual connections in addressing the vanishing gradient problem, promoting quicker convergence during training, and bolstering the model’s ability to generalize effectively to previously unseen data. Simultaneously, the FPN module enriches the models with a mechanism for multi-scale feature fusion.

We compare our proposed method with other state-of-the-art methods, To ensure the fairness of the comparison, the datasets and training parameters remain consistent. In the majority of classification results, our method performs the superior performance. In "NBR" and "+NBE", our method’s F1 score is close to the highest F1 score. These scores surpass the corresponding F1 scores obtained by other methods, highlighting the efficacy of our approach in significantly improving classification accuracy for these specific categories.

Aggregate metrics further corroborate the superiority of our proposed method. Across all considered evaluation criteria, our model achieves an outstanding average F1 score of 92%.

In contrast, competing models such as the baseline CNN only achieve 76%, CNN with residual connections achieve 90%, CNN with both residual and FPN modules achieve 91%, the Transformer achieves 86%, and Transformer with residual connections achieves 89%. This consistent and substantial superiority across a diverse range of signal categories not only validates but further emphasizes the overall effectiveness of our proposed model in the challenging task of lightning signal classification.

2) Comparison with Receiver Operating Characteristic:

To facilitate a comprehensive comparison of diverse model performances, the *receiver operating characteristic* (ROC) methodology was employed. This approach utilizes a graphical plot, depicted in Fig. 8, which showed the diagnostic prowess of a classifier system across varying discrimination thresholds.

In this study, the two specific lightning types: CG-IR in Fig. 8(a) and -NBE in Fig. 8(b) were selected. By comparing the accuracy of state-of-the-art (SOTA) models with ours using their respective ROC curves as a benchmark, our model demonstrated a higher accuracy with areas of 0.98 and 0.99 for the classification of the two lightning types.

In the context of the two aforementioned experiments, firstly, these experiments performed that our proposed model consistently outperforms its counterparts across a diverse spectrum of categories, thereby underscoring its comprehensive superiority in the realm of lightning signal classification. secondly, because of the effectiveness of the Transformer-related model in strategically evaluating the significance of various elements within the input lightning signal sequence. This inherent ability contributes to an overall classification accuracy that surpasses that of CNN and related models.

To further explore the potential performance improvements of the Transformer model, especially when integrated with the multi-scale component, we conducted an ablation experiment. The outcomes of this experiment are presented below.

C. Ablation Study

In this section, we conducted a comprehensive analysis. Firstly, we compared with the Transformer model in terms of accuracy and F1 score. Subsequently, we examined the

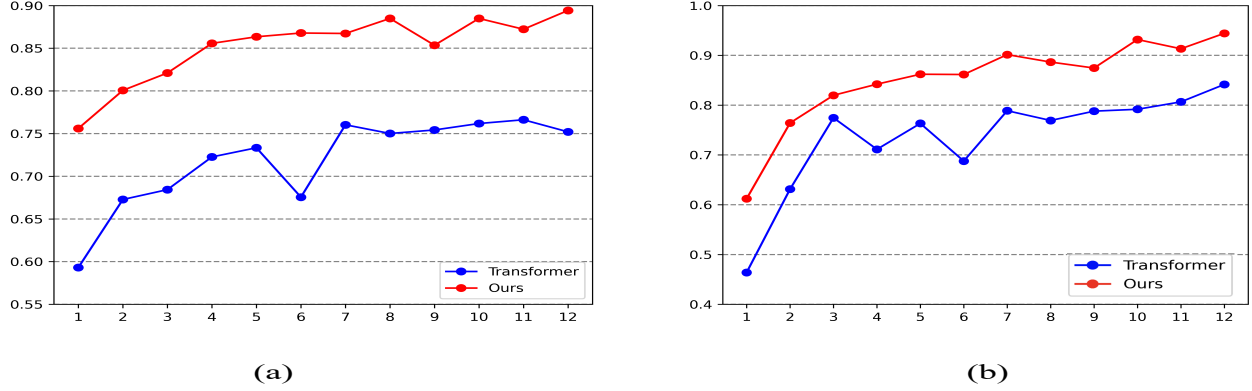


Fig. 9: Comparison of transformer and our method, epoch=12:(a)the results of accuracy;(b)the results of F1 score

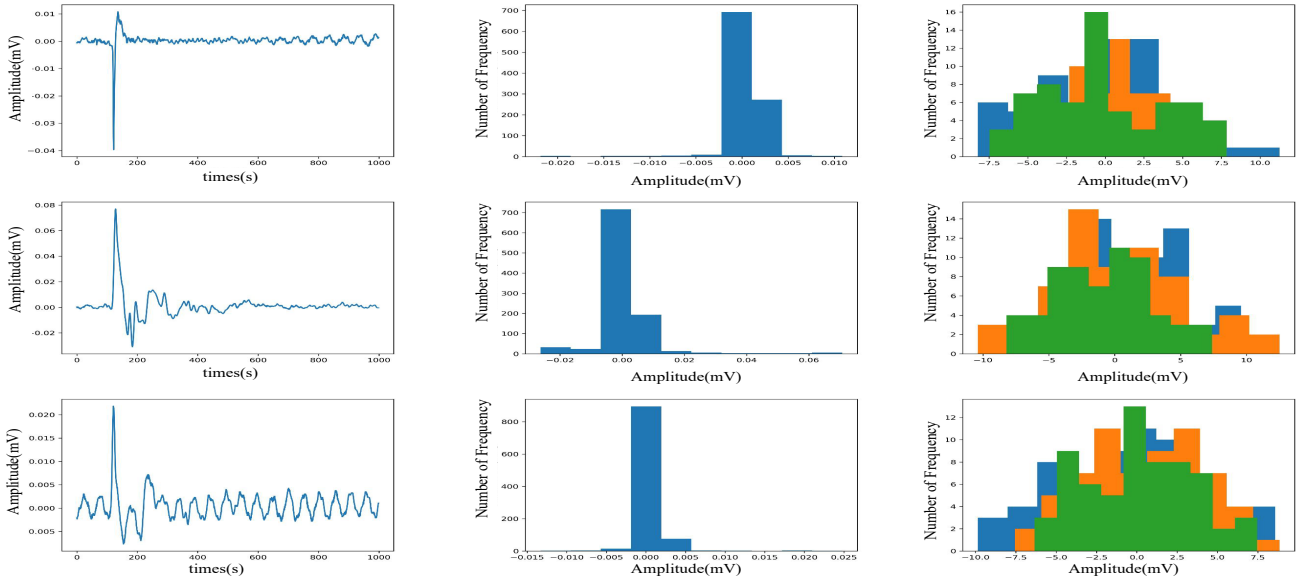


Fig. 10: Different amplitude distributions of lightning signal at different scales: (Left Column)lightning signals; (Middle Column) histogram of lightning signals; (Right Column)histogram of signals at different scales

variations in feature maps within the MSR model at different scales. Finally, we evaluated the dataset’s performance through a five-fold cross-validation procedure, employing experimental datasets.

1) *Model Comparison:* Fig.9 presents a comparative analysis of accuracy and F1 scores attained by the Transformer model and our model across 12 epochs. Our method impressively achieves an accuracy of roughly 85% and F1 score of 90%, markedly outperforming the Transformer model’s accuracy of approximately 75% and F1 score 80%. Evidently, our MSR model plays a pivotal role in the fusion of multi-scale lightning signal features throughout the classification process.

This discrepancy underscores the strength of our model in lightning signal classification. One of the advantages of this feature fusion process is its ability to capture detailed information that might otherwise remain hidden. Lightning signals often exhibit intricate variations across scales, and our model’s capacity to recognize and interpret these subtleties

is contributing to the improvement in classification accuracy, ultimately leading to improvement in classification accuracy.

2) *Multi-scale Visualization Features Map:* Fig. 10 provides a visual representation of distinct amplitude distributions within the lightning signal across a range of scales. This visualization is useful in understanding how the signal’s characteristics evolve as we consider different scales.

The figure shows the gradual transition towards a more uniform amplitude profile as the scales expand. This phenomenon can be attributed to the influence of the multi-scale module within our model architecture. The module plays a pivotal role in harmonizing signal amplitudes and mitigating extreme amplitude disparities between individual lightning pulses.

The flattening of the amplitude serves as a compelling indicator of the efficacy of the multi-scale model. This transformation signifies the model’s proficiency in effectively isolating and accentuating important signal features while reducing the significance of less relevant ones. This improvement in

TABLE III: The F1 score of five-fold cross-validation for different types of classification

K	-CG(%)	CG-IR(%)	NBR(%)	+CG(%)	MP(%)	+PBP(%)	-PBP(%)	-NBE(%)	+NBE(%)	SW(%)	AVG(%)
1	88	88	85	95	97	95	88	94	94	93	92
2	87	87	86	96	94	94	88	94	95	92	91
3	87	87	85	94	93	93	85	92	96	91	90
4	85	86	85	94	92	92	84	92	95	90	90
5	85	84	84	90	88	91	82	93	94	89	88

signal feature discrimination enhances the model’s ability to distinguish between different features.

3) *Five-fold Cross-validation Results:* Table III shows the F1 score of our model across an array of lightning types, each evaluated of individual folds of cross-validation. The F1 scores for most categories such as +CG, +PBP, -NBE, and +NBE consistently exceed 90%, indicating the model’s accuracy in classifying lightning signals. The "AVG(%)" column represents the average F1 score across all five folds for each classification category. This average score consistently demonstrates the model’s strong overall performance, with an average F1 score exceeding 90%.

Thus the table provides a coherent view of our model’s performance across different types of lightning signal classification tasks using a rigorous five-fold cross-validation approach. The model consistently achieves high F1 scores, both at the fold level and in the overall average. That consistency proved our model’s capacity to deliver dependable performance.

TABLE IV: The F1 score of five-fold cross-validation for testing dataset

K	CC(%)	CG(%)	MP(%)	NBE(%)	OTHERS	AVG(%)
1	88	93	83	53	67	83
2	83	94	88	41	33	80
3	86	91	80	23	20	76
4	82	89	70	31	40	74
5	83	89	78	45	64	79

4) *The Results of Testing Dataset:* To show the robustness of our model’s generalization capabilities, the Xingjiang dataset was employed for testing. Utilizing a similar procedure as the experimental dataset, the testing dataset was divided into five categories, each containing approximately 360 instances. The obtained results, displayed in Table IV, showcasing the F1 scores achieved by our model in each fold of cross-validation.

The table shows that despite the smaller scale of the Xinjiang testing dataset compared to the experimental dataset, our model consistently attains an accuracy rate of around 80%. This accuracy rate demonstrates the model’s exceptional ability to maintain classification stability and perform at a high level of accuracy when dealing with datasets of varying sizes and characteristics.

Our model demonstrates versatile adaptability, making it well-suited for real-world applications where lightning signal data can vary in terms of volume, distribution, and signal characteristics. Our model’s capacity to generalize effectively across datasets further solidifies its credibility as a robust and reliable solution for lightning signal classification in diverse environments.

VI. CONCLUSION

Accurate classification of lightning signals holds paramount importance within the realm of VLF lightning signal processing. The advancements in deep learning present a viable avenue for achieving precise lightning signal classification. Beyond the pursuit of classification accuracy, real-world applications necessitate the factors of network simplification and operational stability.

Within this paper, we introduce a multi-scale residual transformer model for VLF lightning waveform classification. This model incorporates a multi-scale residual module, merging low-level and high-level features.

This fusion enhances the model’s ability to identify detailed patterns and capture overall patterns in the signal. Additionally, the module’s proficiency in accommodating features across multiple scales empowers the model to flexibly adapt to signal variations, thereby enhancing its robustness against changing signal characteristics. Integrating this module with a transformer encoder fortified by self-attention mechanisms empowers the model to effectively weigh the significance of different aspects within the input lightning signal sequence, enabling precise classification by focusing on pertinent information.

Through rigorous validation using both open-source and testing datasets, we demonstrate the superior stability and reliability of the proposed network in comparison to conventional CNNs. Furthermore, the prospects for the future application of our model hold the potential to significantly advance our comprehension of lightning signal localization and waveform characteristics. As a result, this paper not only contributes to accurate classification methodologies but also lays the groundwork for broader insights into lightning phenomena.

FUNDING

This work was supported by the Equipment Pre-research Key Laboratory Fund Project(6142403190304),

ACKNOWLEDGMENT

Thanks to the Institute of China Electronics Technology Group Corporation No.22 Research Institute for their data support. The author would also like to thank the reviewers for their helpful feedback, which significantly improved the manuscript.

REFERENCES

- [1] N. Arshad, M. Abdullah, S. Samad, and N. Hatta, "Lightning severity classification technique using very low frequency signal feature extraction," *Journal of Atmospheric and Solar-Terrestrial Physics*, vol. 195, p. 105136, 2019.

- [2] D. Smith, K. Eack, J. Harlin, M. Heavner, A. Jacobson, R. Massey, X. Shao, and K. Wiens, "The los alamos spheric array: A research tool for lightning investigations," *Journal of Geophysical Research: Atmospheres*, vol. 107, no. D13, pp. ACL-5, 2002.
- [3] F. Shen, Z. Wang, Z. Wang, X. Fu, J. Chen, X. Du, and J. Tang, "A competitive method for dog nose-print re-identification," *arXiv preprint arXiv:2205.15934*, 2022.
- [4] H. Kohlmann, W. Schulz, and S. Pedebay, "Evaluation of euclid ic/cg classification performance based on ground-truth data," in *2017 international symposium on lightning protection (XIV SIPDA)*. IEEE, 2017, pp. 35-41.
- [5] A. Nag, M. J. Murphy, K. L. Cummins, A. E. Pifer, and J. A. Cramer, "Recent evolution of the us national lightning detection network," in *23rd International Lightning Detection Conference & 5th International Lightning Meteorology Conference*, 2014.
- [6] R. Said, U. Inan, and K. Cummins, "Long-range lightning geolocation using a vlf radio atmospheric waveform bank," *Journal of Geophysical Research: Atmospheres*, vol. 115, no. D23, 2010.
- [7] V. Cooray, "Propagation effects due to finitely conducting ground on lightning-generated magnetic fields evaluated using sommerfeld's integrals," *IEEE Transactions on Electromagnetic Compatibility*, vol. 51, no. 3, pp. 526-531, 2009.
- [8] J. Hu, Z. Huang, F. Shen, D. He, and Q. Xian, "A bag of tricks for fine-grained roof extraction," in *IGARSS 2023-2023 IEEE International Geoscience and Remote Sensing Symposium*. IEEE, 2023.
- [9] —, "A rubust method for roof extraction and height estimation," in *IGARSS 2023-2023 IEEE International Geoscience and Remote Sensing Symposium*. IEEE, 2023.
- [10] C.-L. Wooi, Z. Abdul-Malek, B. Salimi, N. A. Ahmad, K. Mehranzamir, S. Vahabi-Mashak *et al.*, "A comparative study on the positive lightning return stroke electric fields in different meteorological conditions," *Advances in Meteorology*, vol. 2015, 2015.
- [11] V. Cooray, M. Fernando, C. Gomes, and T. Sorensen, "The fine structure of positive lightning return-stroke radiation fields," *IEEE transactions on electromagnetic compatibility*, vol. 46, no. 1, pp. 87-95, 2004.
- [12] L. Cai, "Ground-based vlf/lf three dimensional total lightning location technology," *Ph. D. dissertation, School Elect. Eng., Wuhan Univ., Wuhan, China*, 2013.
- [13] C. Qiao, F. Shen, X. Wang, R. Wang, F. Cao, S. Zhao, and C. Li, "A novel multi-frequency coordinated module for sar ship detection," in *2022 IEEE 34th International Conference on Tools with Artificial Intelligence (ICTAI)*. IEEE, 2022, pp. 804-811.
- [14] J. Wang, Q. Huang, Q. Ma, S. Chang, J. He, H. Wang, X. Zhou, F. Xiao, and C. Gao, "Classification of vlf/lf lightning signals using sensors and deep learning methods," *Sensors*, vol. 20, no. 4, p. 1030, 2020.
- [15] C. Peng, F. Liu, B. Zhu, and W. Wang, "Lightning waveform classification based on deep convolutional neural network," *Authorea Preprints*, 2022.
- [16] F. Shen, X. Peng, L. Wang, X. Zhang, M. Shu, and Y. Wang, "Hsgm: A hierarchical similarity graph module for object re-identification," in *2022 IEEE International Conference on Multimedia and Expo (ICME)*. IEEE, 2022, pp. 1-6.
- [17] F. Shen, M. Wei, and J. Ren, "Hsgnet: Object re-identification with hierarchical similarity graph network," *arXiv preprint arXiv:2211.05486*, 2022.
- [18] W. Weng, W. Ling, F. Lin, J. Ren, and F. Shen, "A novel cross frequency-domain interaction learning for aerial oriented object detection," in *Chinese Conference on Pattern Recognition and Computer Vision (PRCV)*. Springer, 2023.
- [19] M. Li, M. Wei, X. He, and F. Shen, "Enhancing part features via contrastive attention module for vehicle re-identification," in *2022 IEEE International Conference on Image Processing (ICIP)*. IEEE, 2022, pp. 1816-1820.
- [20] R. Xu, F. Shen, H. Wu, J. Zhu, and H. Zeng, "Dual modal meta metric learning for attribute-image person re-identification," in *2021 IEEE International Conference on Networking, Sensing and Control (ICNSC)*, vol. 1. IEEE, 2021, pp. 1-6.
- [21] C. Peng, F. Liu, B. Zhu, and W. Wang, "A convolutional neural network for classification of lightning lf/vlf waveform," in *2019 11th Asia-Pacific International Conference on Lightning (APL)*. IEEE, 2019, pp. 1-4.
- [22] L. Xiao, W. Chen, Y. Wang, K. Bian, Z. Fu, N. Xiang, H. He, and Y. Cheng, "Towards an interpretable cnn model for the classification of lightning produced vlf/lf signals," 2023.
- [23] F. Hepburn, "Wave-guide interpretation of atmospheric waveforms," *Journal of Atmospheric and Terrestrial Physics*, vol. 10, no. 3, pp. 121-135, 1957.
- [24] H. Wu, F. Shen, J. Zhu, H. Zeng, X. Zhu, and Z. Lei, "A sample-proxy dual triplet loss function for object re-identification," *IET Image Processing*, vol. 16, no. 14, pp. 3781-3789, 2022.
- [25] D. J. Malan, "Physics of lightning," (*No Title*), 1963.
- [26] X. Fu, F. Shen, X. Du, and Z. Li, "Bag of tricks for "vision meet alage" object detection challenge," in *2022 6th International Conference on Universal Village (UV)*. IEEE, 2022, pp. 1-4.
- [27] J. L. Alpert, D. Fligel, and G. Michailova, "The propagation of atmospheric waves in the earth-ionosphere waveguide," *Journal of Atmospheric and Terrestrial Physics*, vol. 29, no. 1, pp. 29-42, 1967.
- [28] R. Challinor, "The phase velocity and attenuation of audio-frequency electro-magnetic waves from simultaneous observations of atmospheric waves at two spaced stations," *Journal of Atmospheric and Terrestrial Physics*, vol. 29, no. 7, pp. 803-810, 1967.
- [29] C. Gao, J. Wang, X. Zhou, F. Xiao, and Q. Ma, "Classification of lightning electric field waveform based on deep residual one-dimensional convolutional network," in *The International Conference on Natural Computation, Fuzzy Systems and Knowledge Discovery*. Springer, 2020, pp. 1648-1659.

- [30] J. Liu, F. Shen, M. Wei, Y. Zhang, H. Zeng, J. Zhu, and C. Cai, "A large-scale benchmark for vehicle logo recognition," in *2019 IEEE 4th International Conference on Image, Vision and Computing (ICIVC)*. IEEE, 2019, pp. 479–483.
- [31] F. Shen, J. Zhu, X. Zhu, Y. Xie, and J. Huang, "Exploring spatial significance via hybrid pyramidal graph network for vehicle re-identification," *IEEE Transactions on Intelligent Transportation Systems*, vol. 23, no. 7, pp. 8793–8804, 2021.
- [32] F. Shen, J. Zhu, X. Zhu, J. Huang, H. Zeng, Z. Lei, and C. Cai, "An efficient multiresolution network for vehicle reidentification," *IEEE Internet of Things Journal*, vol. 9, no. 11, pp. 9049–9059, 2021.
- [33] K. He, X. Zhang, S. Ren, and J. Sun, "Deep residual learning for image recognition," in *Proceedings of the IEEE conference on computer vision and pattern recognition*, 2016, pp. 770–778.
- [34] A. Vaswani, N. Shazeer, N. Parmar, J. Uszkoreit, L. Jones, A. N. Gomez, Ł. Kaiser, and I. Polosukhin, "Attention is all you need," *Advances in neural information processing systems*, vol. 30, 2017.
- [35] A. Einstein, "Zur elektrodynamik bewegter körper," *Annalen der Physik*, vol. 322.
- [36] P. M. Bitzer, H. J. Christian, M. Stewart, J. Burchfield, S. Podgorny, D. Corredor, J. Hall, E. Kuznetsov, and V. Franklin, "Characterization and applications of vlf/lf source locations from lightning using the huntsville alabama marx meter array," *Journal of Geophysical Research: Atmospheres*, vol. 118, no. 8, pp. 3120–3138, 2013.
- [37] F. Shen, X. Shu, X. Du, and J. Tang, "Pedestrian-specific bipartite-aware similarity learning for text-based person retrieval," in *Proceedings of the 31th ACM International Conference on Multimedia*, 2023.
- [38] F. Shen, X. Du, L. Zhang, and J. Tang, "Triplet contrastive learning for unsupervised vehicle re-identification," *arXiv preprint arXiv:2301.09498*, 2023.
- [39] F. Shen, Y. Xie, J. Zhu, X. Zhu, and H. Zeng, "Git: Graph interactive transformer for vehicle re-identification," *IEEE Transactions on Image Processing*, 2023.
- [40] Y. Wang, X. Qie, D. Wang, M. Liu, D. Su, Z. Wang, D. Liu, Z. Wu, Z. Sun, and Y. Tian, "Beijing lightning network (blnet) and the observation on preliminary breakdown processes," *Atmospheric Research*, vol. 171, pp. 121–132, 2016.
- [41] T. Wu, D. Wang, and N. Takagi, "Locating preliminary breakdown pulses in positive cloud-to-ground lightning," *Journal of Geophysical Research: Atmospheres*, vol. 123, no. 15, pp. 7989–7998, 2018.
- [42] A. Krizhevsky, I. Sutskever, and G. E. Hinton, "Imagenet classification with deep convolutional neural networks," *Advances in neural information processing systems*, vol. 25, 2012.
- [43] J. Devlin, M.-W. Chang, K. Lee, and K. Toutanova, "Bert: Pre-training of deep bidirectional transformers for language understanding," *arXiv preprint arXiv:1810.04805*, 2018.
- [44] O. J. Konan, A. K. Mishra, and S. Lotz, "Machine learning techniques to detect and characterise whistler radio waves," *arXiv preprint arXiv:2002.01244*, 2020.
- [45] M. Gołkowski, S. Sarker, C. Renick, R. Moore, M. Cohen, A. Kułak, J. Młynarczyk, and J. Kubisz, "Ionospheric d region remote sensing using elf spheric group velocity," *Geophysical Research Letters*, vol. 45, no. 23, pp. 12–739, 2018.
- [46] P. Hosseini, M. Gołkowski, and V. Harid, "Remote sensing of radiation belt energetic electrons using lightning triggered upper band chorus," *Geophysical Research Letters*, vol. 46, no. 1, pp. 37–47, 2019.
- [47] V. Harid, C. Liu, Y. Pang, A. J. Alvina, M. Gokowski, P. Hosseini, and M. Cohen, "Automated large-scale extraction of whistlers using mask-scoring regional convolutional neural network," *Geophysical Research Letters*, vol. 48, no. 15, p. e2021GL093819, 2021.
- [48] V. Maslej-Krešňáková, A. Kundrát, Š. Mackovjak, P. Butka, S. Jaščur, I. Kolmašová, and O. Santolík, "Automatic detection of atmospheric and tweek atmospheric in radio spectrograms based on a deep learning approach," *Earth and Space Science*, vol. 8, no. 11, p. e2021EA002007, 2021.
- [49] Y. Rapoport, V. Grimalsky, V. Fedun, O. Agapitov, J. Bonnell, A. Grytsai, G. Milinevsky, A. Liashchuk, A. Rozhnoi, M. Solovieva *et al.*, "Model of the propagation of very low-frequency beams in the earth–ionosphere waveguide: principles of the tensor impedance method in multi-layered gyrotropic waveguides," in *Annales Geophysicae*, vol. 38, no. 1. Copernicus GmbH, 2020, pp. 207–230.
- [50] Y. Zhu, P. Bitzer, V. Rakov, and Z. Ding, "A machine-learning approach to classify cloud-to-ground and intra-cloud lightning," *Geophysical Research Letters*, vol. 48, no. 1, p. e2020GL091148, 2021.
- [51] C. J. Davis and K.-H. Lo, "An enhancement of the ionospheric sporadic-e layer in response to negative polarity cloud-to-ground lightning," *Geophysical research letters*, vol. 35, no. 5, 2008.
- [52] S. Kandalgaonkar, M. Tinmaker, J. Kulkarni, and A. Nath, "Diurnal variation of lightning activity over the indian region," *Geophysical research letters*, vol. 30, no. 20, 2003.
- [53] Y.-a. Geng, Q. Li, T. Lin, L. Jiang, L. Xu, D. Zheng, W. Yao, W. Lyu, and Y. Zhang, "Lightnet: A dual spatiotemporal encoder network model for lightning prediction," in *Proceedings of the 25th ACM SIGKDD international conference on knowledge discovery & data mining*, 2019, pp. 2439–2447.
- [54] T.-Y. Lin, P. Dollár, R. Girshick, K. He, B. Hariharan, and S. Belongie, "Feature pyramid networks for object detection," in *Proceedings of the IEEE conference on computer vision and pattern recognition*, 2017, pp. 2117–2125.



Jinghao Sun received the B.Sc degree from Ocean University of China, Qingdao, China, in 2016. He is currently pursuing the Ph.D. degree in Faculty of Information Science and Engineering, Ocean University of China, Qingdao, China.



Tingting Ji received her PhD computer application technology from the Ocean University of China, Qingdao, China, in 2010. She is now with the Teaching Center of Fundamental Courses, Ocean University of China.



Guoyu Wang received the B.S. and M.S. degrees in Ocean Physics from Ocean College of Shandong, Qingdao, China, in 1984 and 1987, respectively. He received Ph.D. degree in Faculty of Electrical Engineering from Faculty of Electrical Engineering, Netherlands, in 2000. He is now a Professor at Ocean University of China. His research interests include pattern recognition image processing and analysis.



Rui Wang received her BS degree in electronic information engineering and her PhD in computer application technology from the Ocean University of China, Qingdao, China, in 2009 and 2014, respectively. She is now at the School of Physics and Electronic Information of Yantai University. Her research interests include image processing and computer vision.